

Development of Water-Based Thermal Insulation Paints Using Silica Aerogel Made From Incineration Ash

Xiaodong Li (✉ li_xiaodong@sp.edu.sg)

Singapore Polytechnic <https://orcid.org/0000-0002-2253-3241>

Yanru Lu

Singapore Polytechnic

Xi Jiang Yin

Singapore Polytechnic

Djati Utomo Handojo

Singapore Polytechnic

Research Article

Keywords: Silica aerogel, Solid waste, Thermal insulation, Water-based paints, Low thermal conductivity, Temperature reduction

Posted Date: July 20th, 2021

DOI: <https://doi.org/10.21203/rs.3.rs-656147/v1>

License:   This work is licensed under a Creative Commons Attribution 4.0 International License.

[Read Full License](#)

Abstract

Building insulation plays an important role in energy consumption reduction for sustainable buildings. By applying an efficient insulation, the energy used to keep the building cool or warm can be saved significantly. In this work, we have developed a sustainable method for fabrication of silica aerogel (SA) micro powder from solid waste ashes collected from waste-to-energy incineration plants. The fabricated SA has a low thermal conductivity of 0.025 W/mK, high surface area of 786 m²/g and high porosity of 96.36%. It has been mixed into water-based paints to develop a high efficient thermal insulation paint with improved thermal insulation properties. Different percentage of SA were mixed into the paint samples to prepare the silica aerogel thermal insulation paint (SATIP) and their physical properties were studied. The SATIP samples were then coated on cement board substrates. The thermal conductivity, water resistance, and insulation performance of the samples were investigated and evaluated systematically. The thermal conductivity results demonstrate that SA additive could significantly improve the thermal insulation properties of the paint. By adding 20 vol% of SA into the SATIP, it achieves up to 12 °C surface temperature reduction improvement compare to the one without SA on the heated plate at 60 °C, and 1 °C in-chamber temperature reduction with external temperature of 44.6 °C. The results demonstrated a promising and high efficient thermal insulation paint with silica aerogel which has a great potential for application in sustainable and green buildings for energy saving.

Statement Of Novelty

Low cost and high performance silica aerogel has been successfully fabricated from waste ashes collected from incineration plants. Through the method developed, the production cost of the traditional expensive silica aerogel can be reduced by 50%, making the novel material affordable by building industry. By adding fabricated silica aerogel into a normal paint, its thermal conductivity is reduced and thermal insulation performance is improved. With 20 vol% of silica aerogel additive, the paint shows up to 12 °C surface temperature reduction improvement on the heated plate at 60 °C and 1 °C in-chamber temperature reduction with external temperature of 44.6 °C compare to the one without additive. The results demonstrated a novel method for solid waste recycling and application.

Introduction

Building insulation plays an important role on energy consumption saving for green buildings, especially for those tropical countries located near the equatorial region, such as Singapore. An efficient and high performance building insulation is able to save the building energy consumption by up to 80%, while at the same time, it offers improved conditions for building residents and users to live and work with comfort. Exterior coating of the building is one of such functional insulation materials that create a protection barrier between the internal and external environments of a building.

To promote the use of energy-efficient exterior coatings for buildings, solar reflective paints have been developed to achieve better building energy efficiency and mitigate the urban heat island effect [1–3]. Its

low k-value, high thermal emissivity, and high solar reflectance reduces direct sun energy absorption, hence a cool energy saving is achieved [1, 2].

However, there are also some disadvantages of the solar reflective paint. Firstly, different solar reflective paints with different technology yield same total solar reflectance (TSR) and solar reflectance index (SRI) readings, may have different performance of temperature reduction of ranging from 2 to 11 °C [1–5]. The good product has lower k-Value (slower heat transfer from external to internal surface) and higher thermal emissivity (faster cooling of heat built-up on external surface) as compared to the other one having the same TSR & SRI value. The good and the bad are mixed, which are solely based on solar reflectivity. Secondly, it is color sensitive, light color paint may have better performance than the dark color paint [6–8]. Lastly, it will lose function after it is re-painted and coated by other normal paint.

An alternative cool coating is using the insulation technology. The advantages of the insulative coating is low k-value, but colour insensitive which means both the light and dark colour paint have the same excellent insulation performance. The problem is that it may require much higher thickness to achieve high insulation properties compared to the solar reflective paints as the thermal conductivity of conventional insulative additives are relatively high. In this study, we use the super insulation material, silica aerogel, as the insulative additives. Silica aerogel has the lowest thermal conductivity among all the solid insulation materials in the world [9–11], and even better than the still air. It consists of amorphous silica structure with over 90% of air, and thus, is considered to be the world's lightest solid material. Its porous structure also allows it to be breathable with fresh air passing through it. The addition of silica aerogel into building materials can significantly lower their thermal conductivity or k-value and achieve previously unattainable thermal performance. By incorporating aerogel in paints, the thickness of the coatings can be significantly reduced to micrometers while still achieving excellent building energy efficiency.

The only thing which hinders its wide application is the cost of the novel material. It was even more expensive than the gold. Although its price is keeping dropping along the years, the building sectors still not be able to afford it. Here, in this work, low cost and high performance aerogel powder has been synthesized by using the solid waste material, incineration waste ashes. The cost can be much reduced.

Experimental Section

SA granulate was fabricated from incineration waste ashes by two steps, and the details are described in previous work [12]. The incineration ash was received from Sembcorp Industries. The first step was the production of sodium silicate or water glass solution. Firstly, the incineration waste ashes underwent leaching process with 1M Hydrochloride (HCl) solution for 3 hours to remove the contaminated metal elements, such as iron. Secondly, the solid powders were collected by vacuum filtration. Thirdly, silicon was extracted by refluxing with 2M sodium hydroxide solution for 24 hours to form the water glass solution. After the production of the water glass solution, the second step was the fabrication of SA granulate. Firstly, the water glass solution was diluted to silica sol with a silicon content of around 6 wt%

with deionized water. 1M HCl solution was added drop by drop under stirring until the pH value of 8 ~ 11 was reached. The gelation of the solution completed within 3 ~ 5 min. The gel was then left for aging for 3 hours at room temperature and followed by crushing into small pieces. The surface modification of the gel was done by adding isopropanol, n-Hexane and trimethylsilyl chloride (TMCS) into the gel under stirring for 3 hours. The volume ratio of gel, isopropanol and n-Hexane was kept at 10:3:6. The molar ratio of silica and TMCS was chosen to be 1:4. The gel after treatment could float on top of the liquid phase. Finally, the SA granulate was obtained by removing the liquid and drying the gel at 50 °C for 1 hour and at 150 °C for 1 hour in an oven.

Fine SA powder was then prepared by ball milling the SA granulate and its particle size was controlled by using a 100 µm sieve. The SA powder was then mixed into a white color exterior paint (Weatherbond, Nippon Paint, Singapore) under vigorous stirring to obtain silica aerogel thermal insulation paint (SATIP). The SA content in the paint was adjust from 0–20% in volume ratio. The paint was then coated onto cement board substrate with thickness of about 200 ± 20 µm.

The structure of the SA powder was characterized by X-ray diffraction (XRD, D8-ADVANCE, Bruker, USA). The surface area of the SA powder was determined by nitrogen physisorption measurements with a Nova 2200e (Quantachrome, USA). The sample was degassed in vacuum at 80 °C for 24 h before measurement. The thermal gravimetric analysis (TGA) test was performed by a TGA/DSC Simultaneous Thermal Analyzer (Mettler Toledo, Switzerland) to study the thermal stability of the aerogel. The specimen was heated from room temperature to 900 °C at a rate of 10 °C/min in argon. The viscosity of the paint were measured by a digital viscometer (TQC Sheen, Netherlands). The thickness of the paint samples was measured by a coating thickness gauge (Elcometer, Singapore) and the hydrophobicity were tested by an automatic contact angle meter (Analytical Technologies, Singapore). The thermal conductivity was determined by a C-Therm TCi Thermal Conductivity Analyzer (C-Therm Technologies, Canada) using the modified transient plane source method under ambient conditions. Reflectance was measured from 250–2250 nm by using UV-Vis-NIR spectrophotometer (Shimadzu, Japan). The thermal insulation performance of the SATIP was measured by heating the paint coated cement boards on a hotplate, the temperature of the hotplate was set to around 60 °C and the temperature of the both sides of the paint samples were recorded concurrently by digital thermometers. A simulation thermal insulation testing was also performed, the setup was shown in Fig. 1. An infrared lamp power of 300W for a sun light simulation directly illuminated onto the front of the samples. The temperature on the surface of the paint was monitored by an IR thermometer and the temperature inside the chambers were recorded by digital thermometers. The heat transfer from the external to the internal of the chambers was not affected by convection from the heat source.

Results And Discussion

Figure 2a shows the incineration ash as received, and Fig. 2b and c show the images of the fabricated SA granulate and SA powder after ball milling, respectively. The SA powder is liquid-like and has a slight change in color from white to translucent after ball milling. The color change is attributed to the low

density and high porosity of the SA powder. Its density is measured to be around 0.08 g/ml and porosity is calculated to be 96.36%. Its thermal conductivity is measured to be around 0.025 W/mK.

The XRD pattern of SA powder is shown in Fig. 3. The XRD result shows a broad peak between 20° to 30° without any sharp peaks, which indicates that the SA powder is fabricated in amorphous structure [13]. Thus, the safety of the SA powder can be assured with no or minimal chronic effects for application in building insulation [14].

Fig. 4 shows typical nitrogen adsorption and desorption isotherms of fabricated SA powder. The pore size distribution of the silica aerogel calculated from the adsorption and desorption data, which leads to values of the core pore radius, is shown in Fig. 5 (a and b). The Barrett-Joyner-Halenda (BJH) adsorption average pore radius ($2V/A$) is 82.3 Å, while the BJH desorption average pore radius ($2V/A$) is 64.1 Å. The BET surface area is 786 m²/g. The average pore width ($4V/A$ by BET) is 20 nm with a narrow distribution and the BJH cumulative pore volume of pores between 0.85 nm and 150 nm radius is about 3.9 cm³/g. The surface area of the fabricated SA powder is 786 m²/g.

Figure 6 shows the result of the TGA of the fabricated SA powder. TGA shows the thermal stability of the fabricated SA powder. A slight weight loss is observed on the curve at 75–125 °C, which may be attributed to the evaporation of water trapped by the SA. The water content is less than 2%. A 9% weight loss is found when increasing the temperature to 375 °C to 775 °C. The onset temperature is around 418 °C at which the SA exposed to heat undergo the degradation. This is due to the oxidation of silicon-carbon bond (Si-CH₃) to silanol groups (Si-OH) and evaporation of organic components at the SA surface [15]. And after the heat treatment, the hydrophobic SA is converted into hydrophilic SA.

The workability of the paint was measured through viscosity. Different percentage of silica aerogel from 5–20% in volume was added into the paint, and the viscosity result is shown in Fig. 7. It shows that there is a sharp increase in viscosity after adding aerogel and the viscosity further increases with the increase of the aerogel content from 5–20%. The adding of hydrophobic SA powder can reduce the agglomeration problem of the nano-sized filler, and at the same time, enhance the interfacial interactions [16]. This enhancement is mainly attributed to the improved mechanical anchoring between the porous SA powder and the paint matrix by mechanical interlocking generated by the pores.

The adding of SA powder not only affects the viscosity of the paint, but also contributes in the shift of surface energy [17]. The contact angle of the paint with aerogel additives were also measured and the results are shown in Fig. 8. Figure 8 shows the influence of surface energy on wettability. As the SA content increases from 5–20%, the contact angle increases steadily, from 52.47 degrees to 64.38 degrees, indicating a better water repellence of the paint, improved self-cleaning property and mildew growth prevention. The aging and service life of the paint can thus be prolonged. This improvement is due to the addition of hydrophobic aerogel powder. The increase of the hydrophobic SA content corresponding to the increase of contact angles indicates that chemical is mainly responsible for the increase in hydrophobicity rather than surface roughness effect.

Figure 9 shows the thermal conductivity of paints with different SA content. As shown in Fig. 9, the thermal conductivity of the paints decreases with the increase of SA content owing to its superior thermal conductivity (0.025 W/mK). Thus, the enhancement of this property is beneficial for reduction of the conduction and dissipation of heat [18]. As a result, the thermal insulation properties would be improved. These findings can be used to demonstrate the effects of SA addition on the thermal insulation performance of paints. However, due to low density of SA powder, the volume of added SA is limited by 20 %. When the content of the SA is further increased, the defects such as cracks and small lumps will be generated from the dried coating.

The thermal insulation performance of the SATIPs were measured by putting the samples onto a hotplate, as shown in Fig. 10a, the temperature of the hotplate was set to around 60 °C. A paint sample without SA additive was tested at left side of the hotplate as a reference for comparison, while SATIP samples with different SA content was tested at the right side of the hotplate. The IR images clearly shows that the surface temperature of the sample with SA additive is lower than that of the sample without additive, as shown in Fig. 10b. The surface temperature of the both sides of the samples was then measured concurrently by using two thermocouples. The temperature reduction was calculated by subtracting the bottom temperature from the top temperature of the samples. Figure 10c shows the temperature reduction of SATIPs with different SA content. As can be seen from the curve, the temperature reduction increases with the increase of the SA content, demonstrating the improved insulation performance by adding SA additive. Up to 12 °C improvement in temperature reduction is achieved compare to the one without SA. The trend is in line with the trend of the thermal conductivity of paints with different SA content.

Figure 11 shows the spectral reflectance of paints with different SA content. It can be seen that there is no obvious difference in the spectrum from visible to near infrared among all paints with 0–20% SA additive. The photons appear not to be interacting with the particles as the size of the SA particles are much larger than the wavelength of the incident light [19]. The reflectance is contributed by the original pigment in the white paint. This spectral reflectance results indicates that the improvement of the thermal insulation performance of the SATIP is attributed to the thermal conductivity reduction from SA additive instead of the heat reflectance of paints with additive.

Figure 12 shows the thermal insulation performance of paint without (left) and with (right) 20% SA additive. The external surface temperature of the samples were monitored by using an IR thermometer. As shown in Fig. 12, the SATIP with 20% SA has better thermal insulation with the temperature difference of 1 °C under the external temperature of 44.6 °C compared with the paint without SA. This insulation performance improvement is mainly due to the thermal conductivity reduction contributed by SA additive. By adding SA into paint, the thermal conduction and convection of paint is reduced.

Conclusions

SA powder has been prepared from industry incineration waste ashes and characterized with a density of 0.08 g/ml, surface area of 786 m²/g, pore size of 20 nm, and porosity of 96.36%. By adding SA powder into paints, their thermal conductivities are decreased and thermal insulation performance are improved. The result also shows that the improvement of thermal insulation is attributed to thermal conductivity reduction instead of heat reflection. The SATIP with 20% SA additive demonstrated better thermal insulation performance with up to 12 °C improvement in temperature reduction compare to the one without SA on the heated plate at 60 °C, and 1 °C in-chamber temperature reduction under the external temperature of 44.6 °C.

Declarations

Funding

This work was funded by the Singapore Ministry of Education Translational R&D and Innovation Fund (MOE2018-TIF-1-G-031).

Conflicts of interest/Competing Interests

The authors declare that they have no competing interests.

Availability of data and materials

All data generated or analyzed during this study are included in this published article.

Code availability

Not applicable.

Authors' contributions

All authors contributed to the study conception and design. Material preparation, data collection and analysis were performed by Yanru Lu and Xiaodong Li. The first draft of the manuscript was written by Xiaodong Li and all authors commented on previous versions of the manuscript. All authors read and approved the final manuscript.

Ethics approval

Not applicable.

Consent to participate

Not applicable.

Consent for publication

Not applicable.

Acknowledgement

This work was supported by the Singapore Ministry of Education Translational R&D and Innovation Fund (MOE2018-TIF-1-G-031).

References

1. Synnefa A., Santamouris M. , Livada I.: A study of the thermal performance of reflective coatings for the urban environment. *Sol. Energy*. **80**, 968-981 (2006)
2. Rosenfeld A.H. , Akbari H. , Bretz S. , Fishman B.L. , Kurn D.M. , Sailor D. , Taha H.: Mitigation of urban heat islands: materials, utility programs, updates. *Energy Build.* **22**, 255-265 (1995)
3. Simpson J.R., McPherson E.G.: The effects of roof albedo modification on cooling loads of scale model residences in Tucson Arizona. *Energy Build.* **25**, 127-137 (1997)
4. Hernández-Pérez I., Álvarez G., Xamán J., Zavala-Guillén I., Arce J., Simá E.: Thermal performance of reflective materials applied to exterior building components—A review. *Energy and Buildings*. **80**, 81-105 (2014)
5. Malza Sebastian, Krenkelb Walter, Steffensa Oliver: Infrared reflective wall paint in buildings: Energy saving potentials and thermal comfort. *Energy and Buildings*. **224**, 110212 (2020)
6. Kai L. Uemoto, Neide M.N. Sato, Vanderley M. John: Estimating thermal performance of cool colored paints. *Energy and Buildings*. **42**, 17–22 (2010)
7. Gonome H., Nakamura M., Okajima J., Maruyama S.: Artificial chameleon skin that controls spectral radiation: Development of chameleon cool coating (C3). *Sci. Rep.* **8**, 1196 (2018)
8. Song J., Qin J., Qu J., Song Z., Zhang W., Xue X., Shi Y., Zhang T., Ji W., Zhang R., Zhang H., Zhang Z., Wu X.: The effects of particle size distribution on the optical properties of titanium dioxide rutile pigments and their applications in cool non-white coatings. *Sol. Energy Mater. Sol. Cells*. **130**, 42–50 (2014)
9. Fricke, J. and Emmerling, A.: Aerogels—Preparation, Properties, Applications. *Structure and Bonding*. **77**, 37 (1992)
10. Hrubesh, L.W.: Aerogels: The World's Lightest Solids. *Chemistry & Industry* , **17**, 824. (1990)
11. Hüsing, N. and Schubert, U.: Aerogels—Airy Materials: Chemistry, Structure, and Properties. *Angewandte Chemie International Edition*. **37**, 22 (1998)
12. Lu Yanru, Li Xiaodong, Yin Xijiang, Utomo Handojo Djati, Tao Nengfu, Huang Hai: Silica Aerogel as Super Thermal and Acoustic Insulation Materials. *Journal of Environmental Protection*. **9**, 295-308 (2018)
13. Khedkar Mangesh V., Somvanshi Sandeep B., Humbe Ashok V., Jadhav K.M.: Surface modified sodium silicate based superhydrophobic silica aerogels prepared via ambient pressure drying process. *Journal of Non-Crystalline Solids*. **511**, 140-146 (2019)

14. Nafisi S., Schäfer-Korting M., Maibach H.I.: Measuring Silica Nanoparticles in the Skin. In: Humbert P., Fanian F., Maibach H., Agache P. (eds) Agache's Measuring the Skin. Springer, Cham. 1141-1164 (2017) https://doi.org/10.1007/978-3-319-32383-1_44
15. Sarawade P.B. , Kim J.-K. , Hilonga A. , Quang D.V. , Jeon S.J. , Kim H.T.: Synthesis of sodium silicate-based hydrophilic silica aerogel beads with superior properties: effect of heat-treatment. J. Non-Cryst. Solids. **357**, 2156-2162 (2011)
16. Salimian, S.; Zadhoush, A.; Mohammadi, A., A Review on New Mesostructured Composite Materials: Part I. Synthesis of Polymer-Mesoporous Silica Nanocomposite. Journal of Reinforced Plastics and Composites. **37**, 441-459 (2018)
17. Aksu Rana, Saygi Berrin: Investigation of Silica Aerogels Effect on Paint Characteristics. European Journal of Engineering and Natural Sciences. **3**, 139-146 (2019)
18. He Fang, Qi Zhentao, Zhen Wei, Wu Juying, Huang Yuhong, Xiong Xianwen, Zhang Ruizhu: Thermal Conductivity of Silica Aerogel Thermal Insulation Coatings. Int J Thermophys. **40**, 92 (2019)
19. R.M. Nelson, B.W. Hapke, W.D. Smythe, L.J. Spikler The opposition effect in simulated planetary regoliths. Reflectance and circular polarization ratio change at small phase angle Icarus. **147**, 545-558 (2000)

Figures

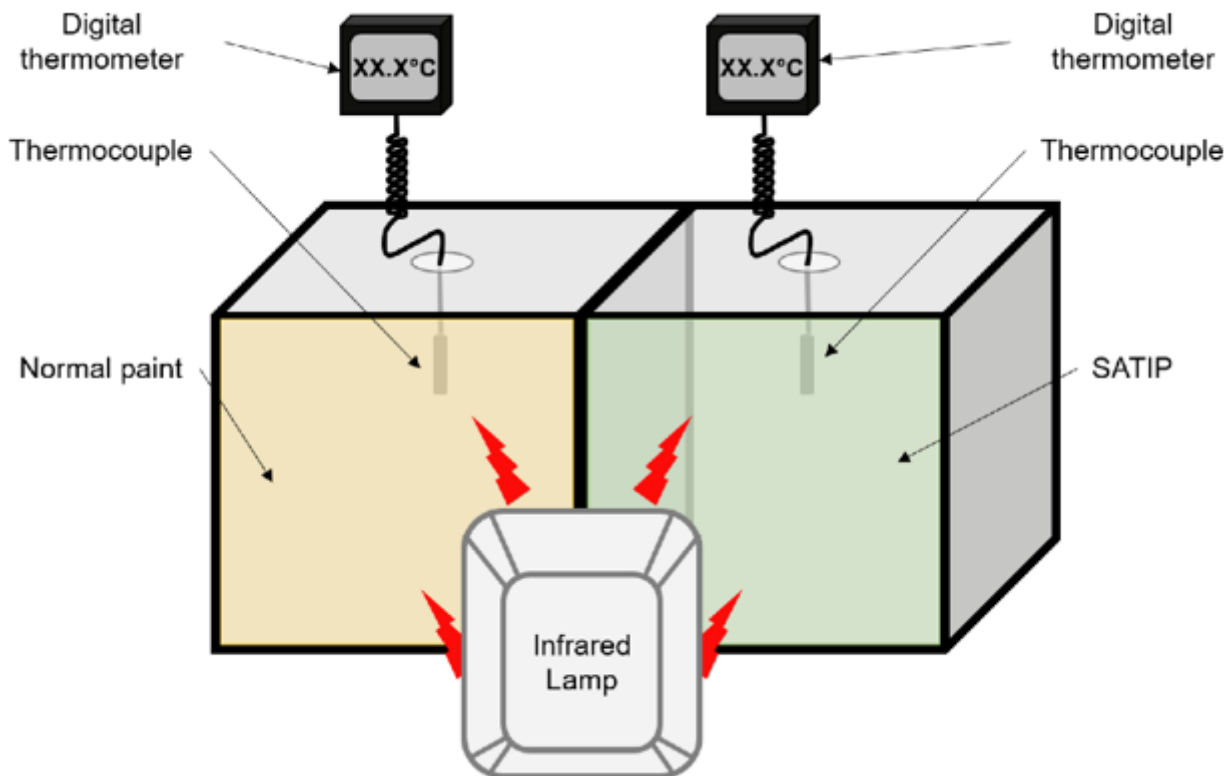


Figure 1

Experimental setup scheme for testing thermal insulation performance

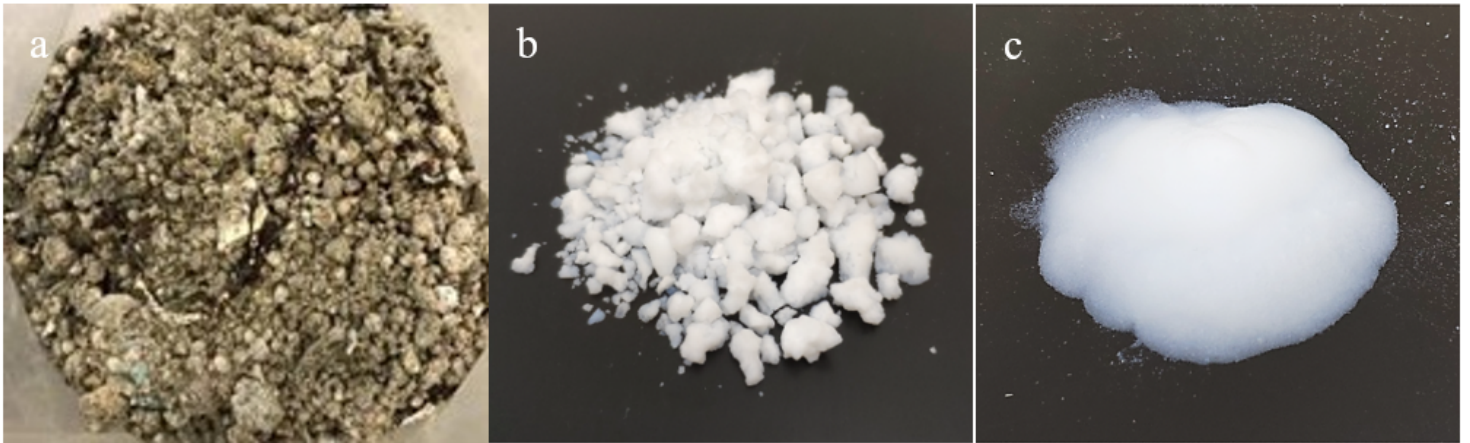


Figure 2

Photos of incineration ash (a) and fabricated SA granulate (b) and powder (c)

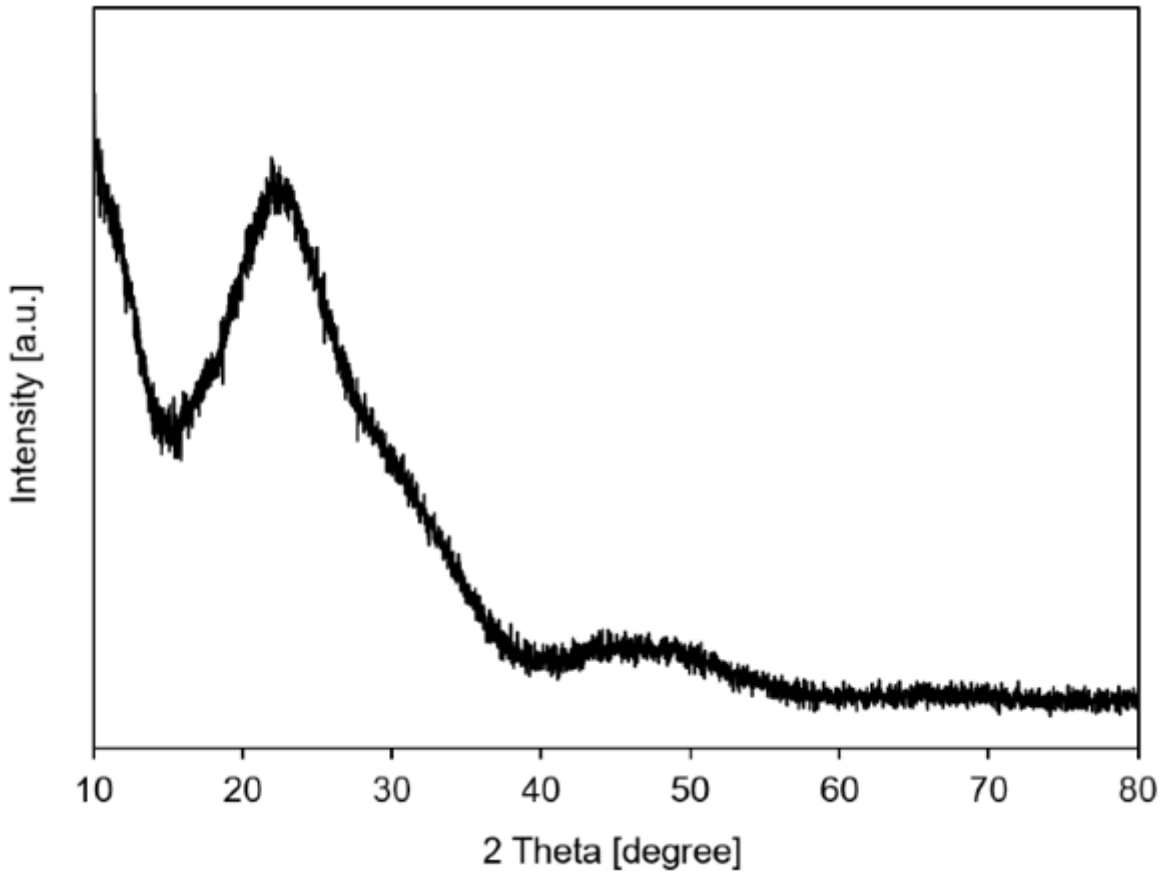


Figure 3

XRD pattern of SA powder

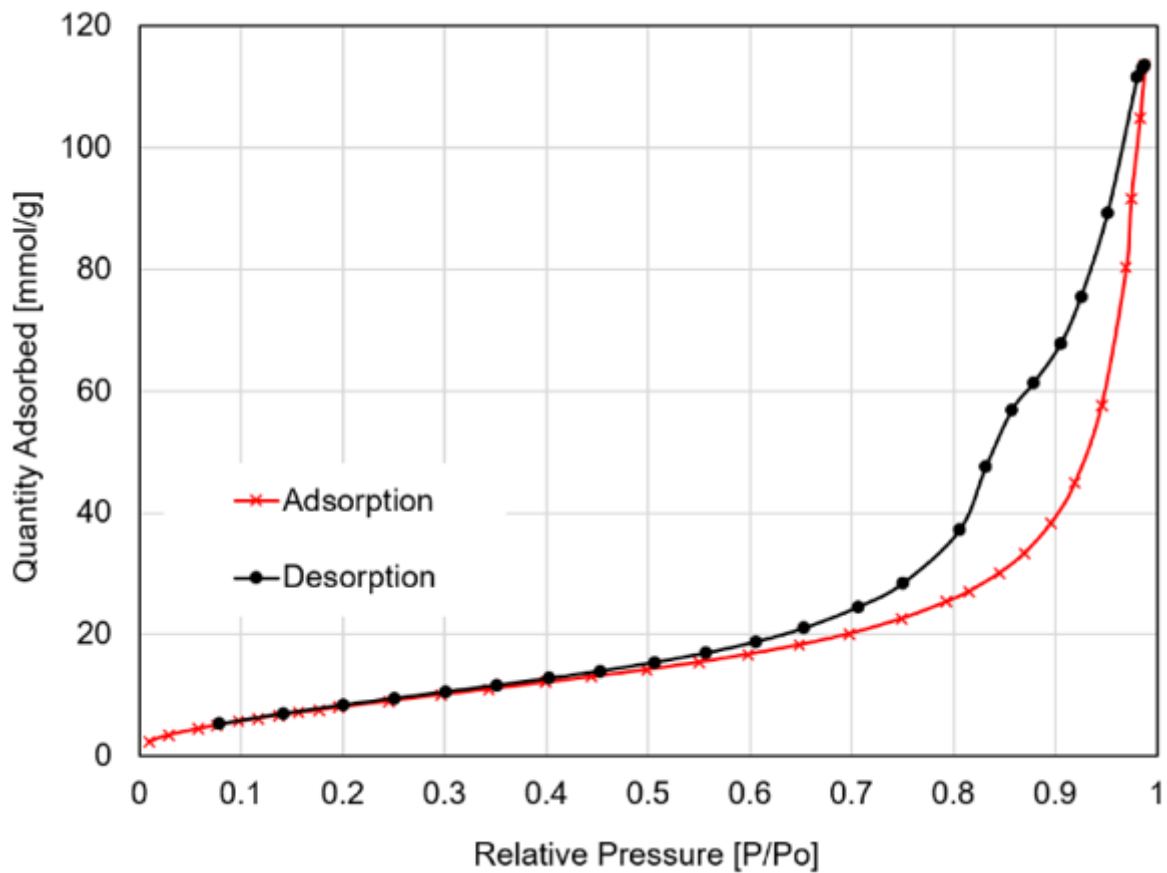


Figure 4

N₂ adsorption and desorption isotherm of fabricated SA powder at 77K

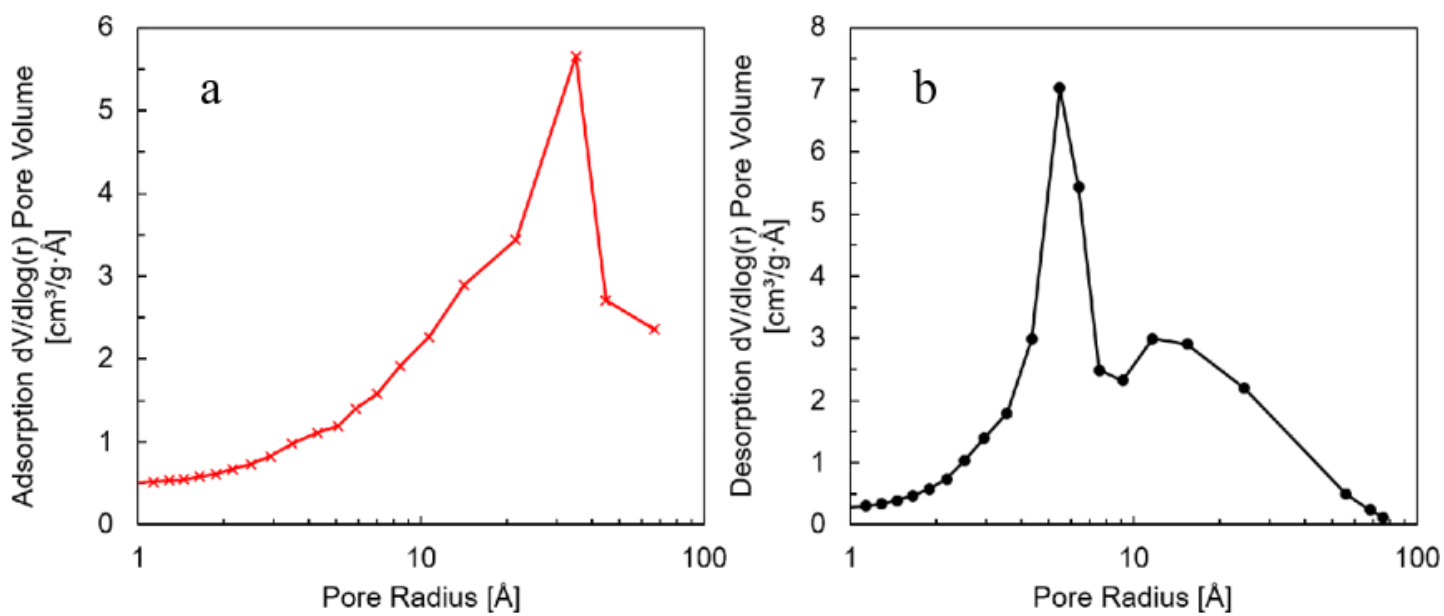


Figure 5

Pore volume distribution $dV/d\log(r)$ calculated from adsorption data (a) and desorption data (b) of Fig. 4

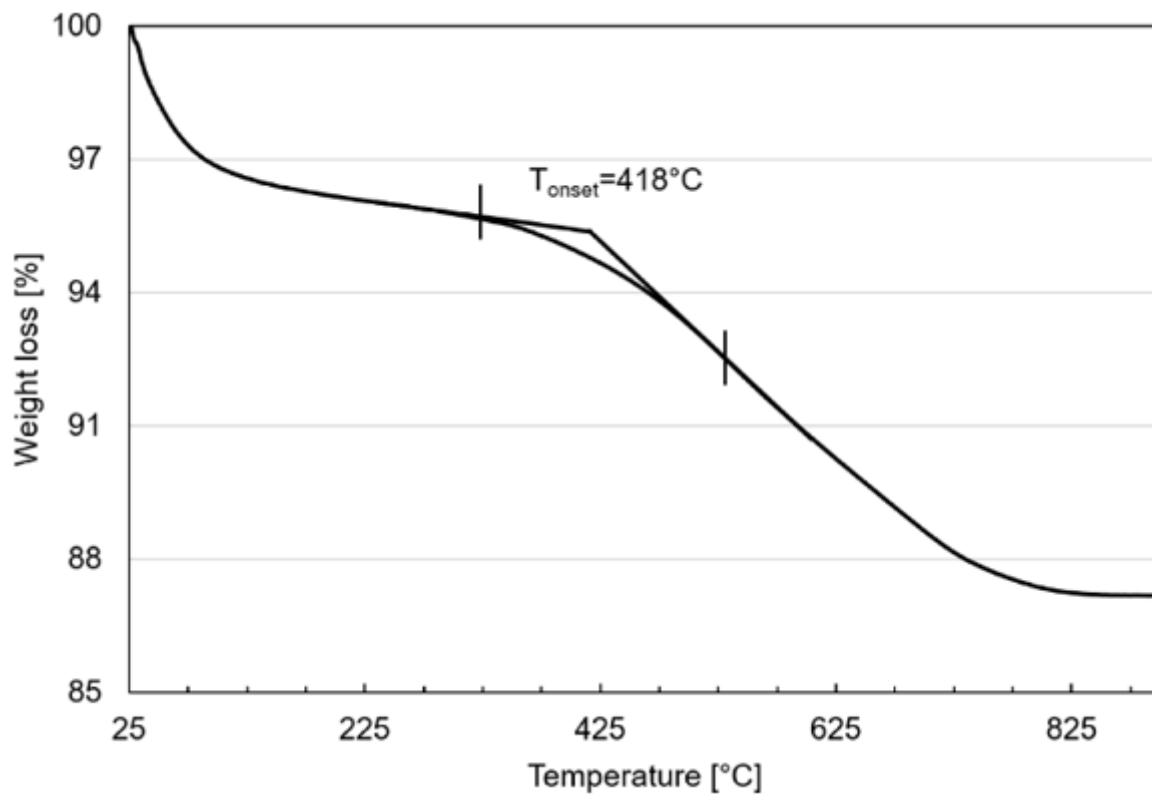


Figure 6

TGA curve for the fabricated SA powder

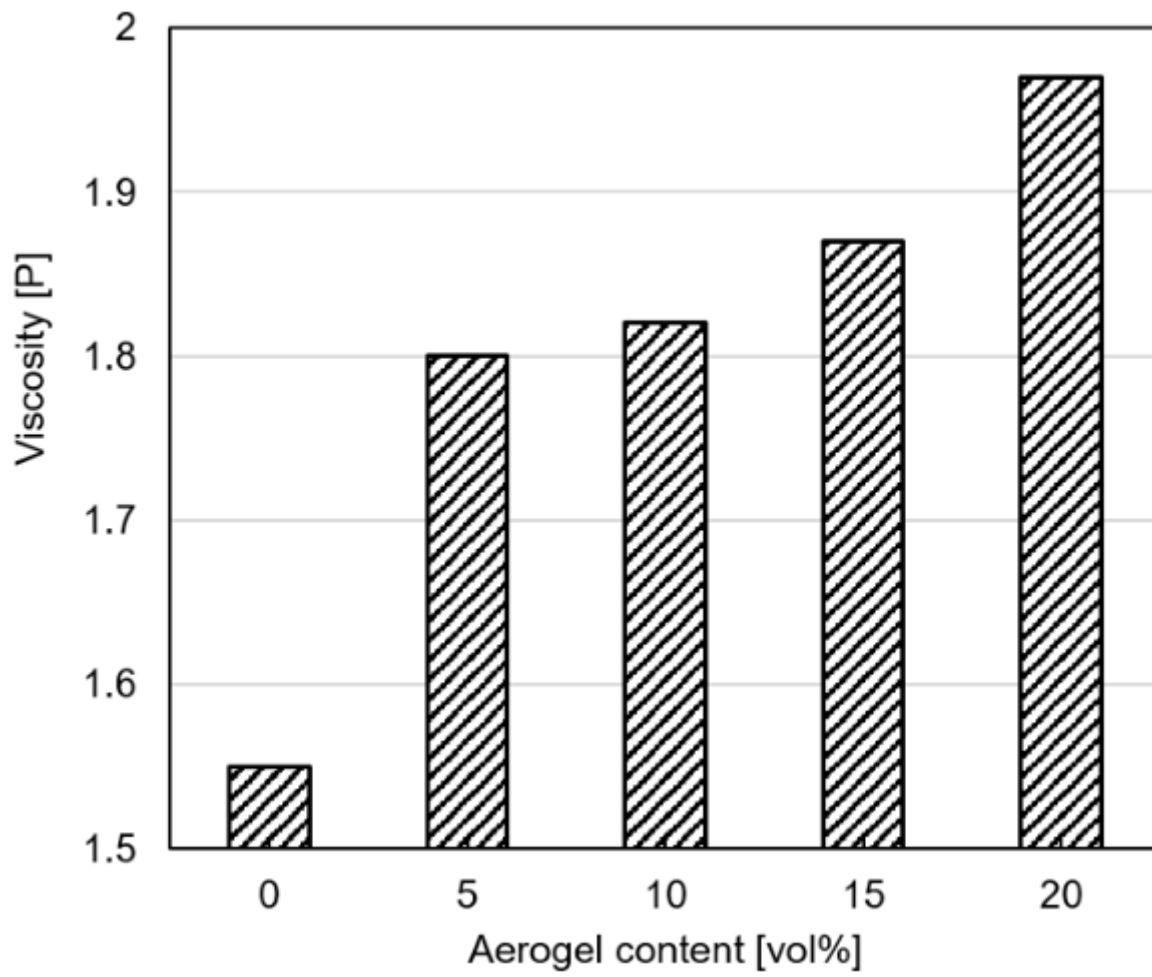


Figure 7

Viscosity of paints with different SA content

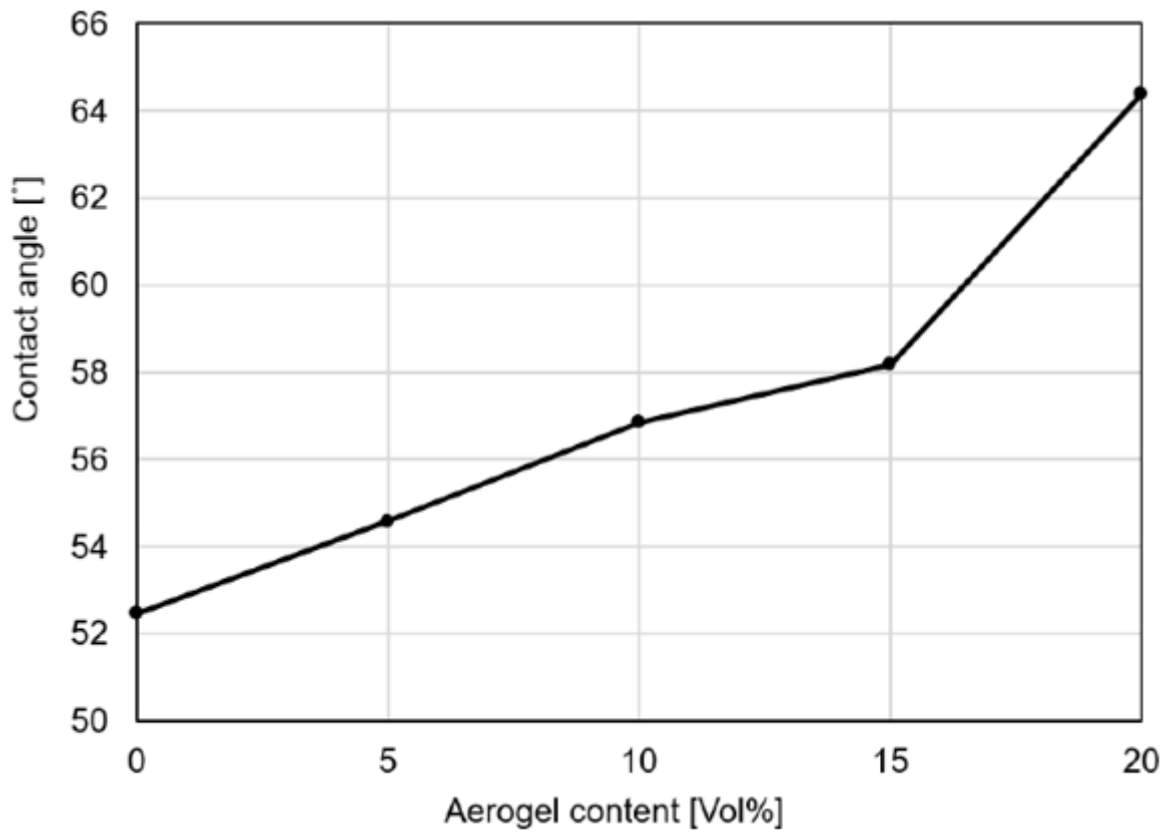


Figure 8

Contact angle of paints with different SA content

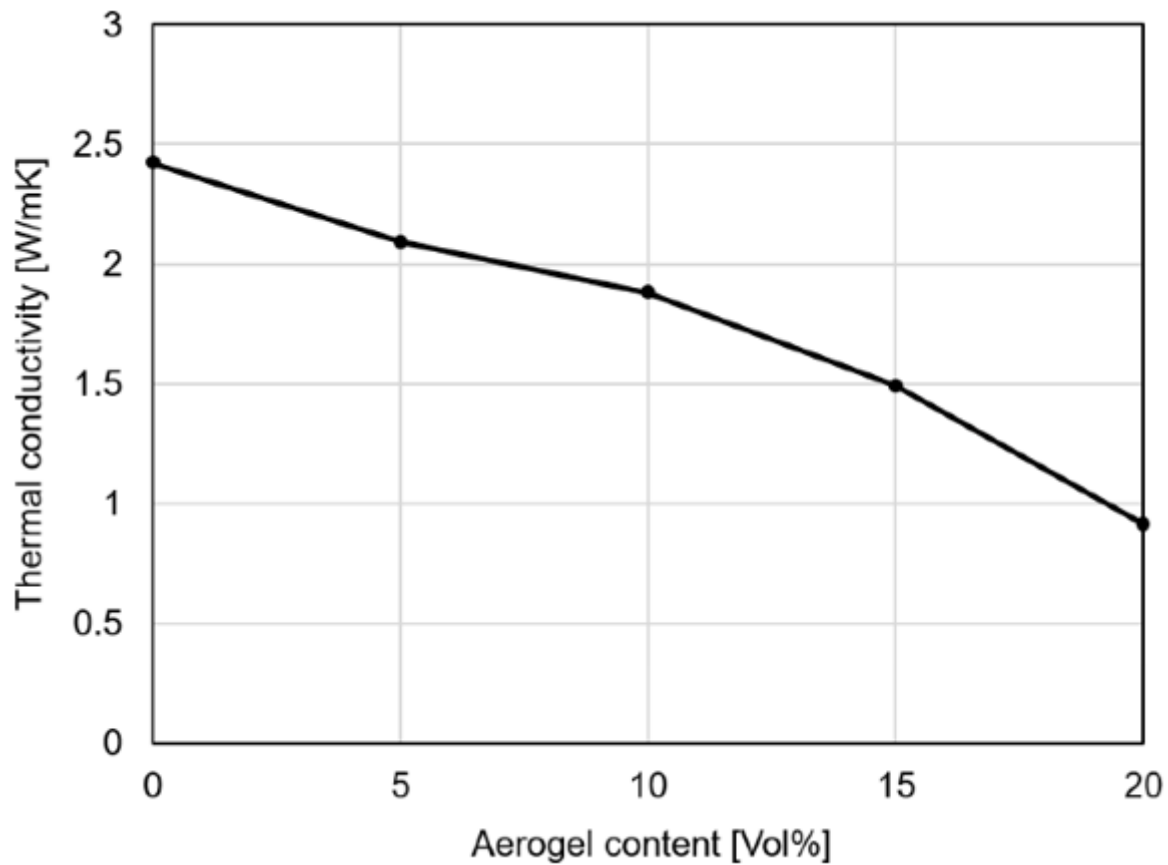


Figure 9

Thermal conductivity of paints with different aerogel content

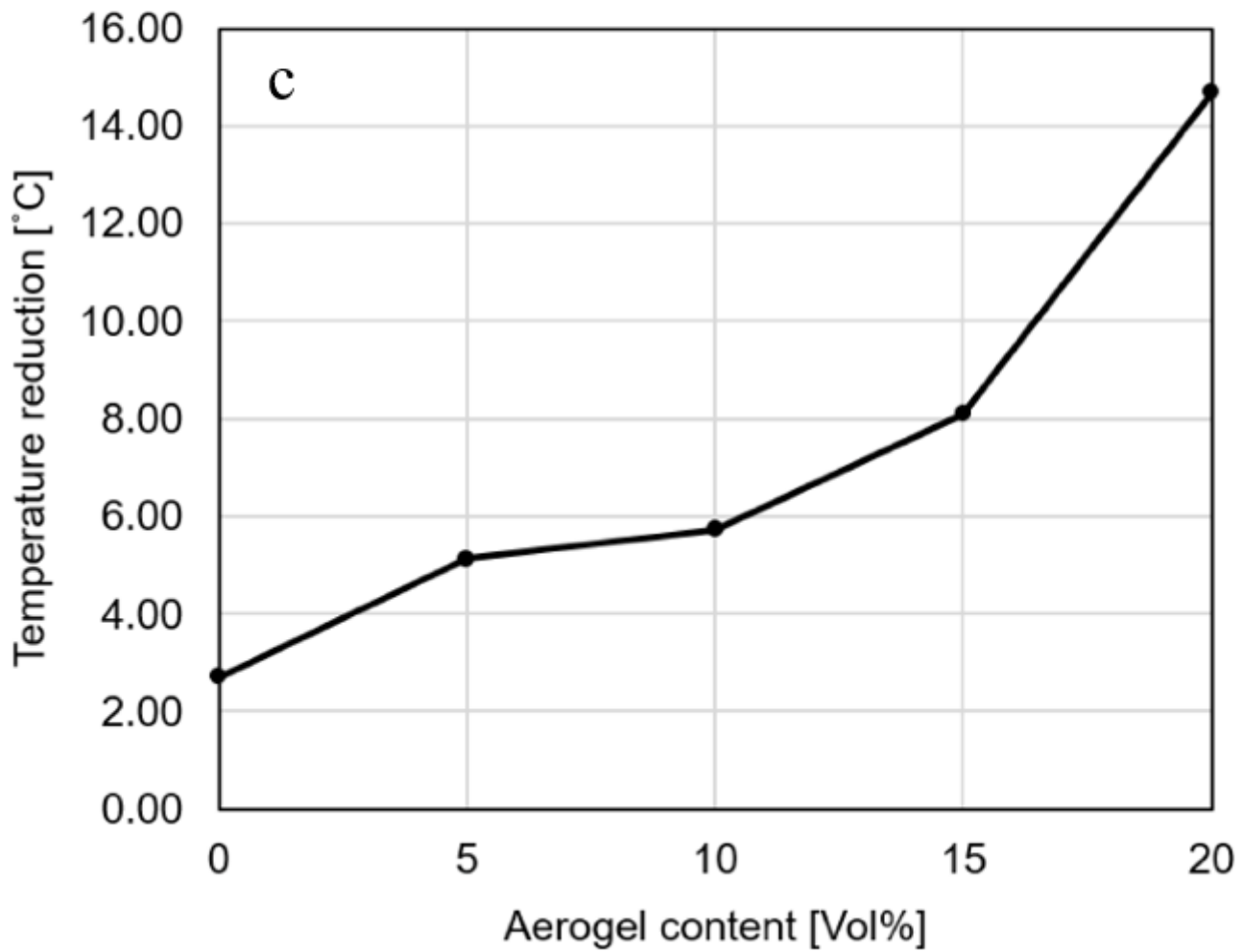
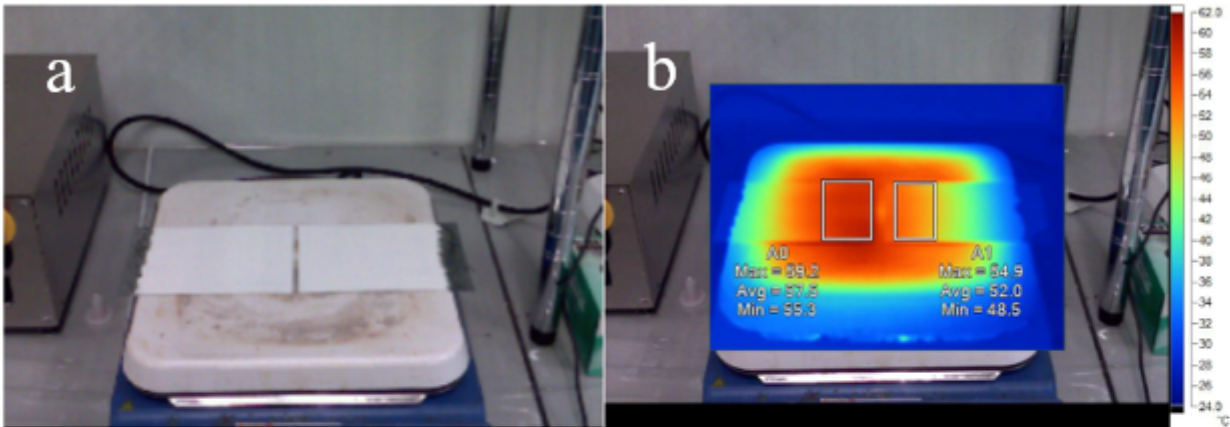


Figure 10

Temperature reduction test of paints with different SA content

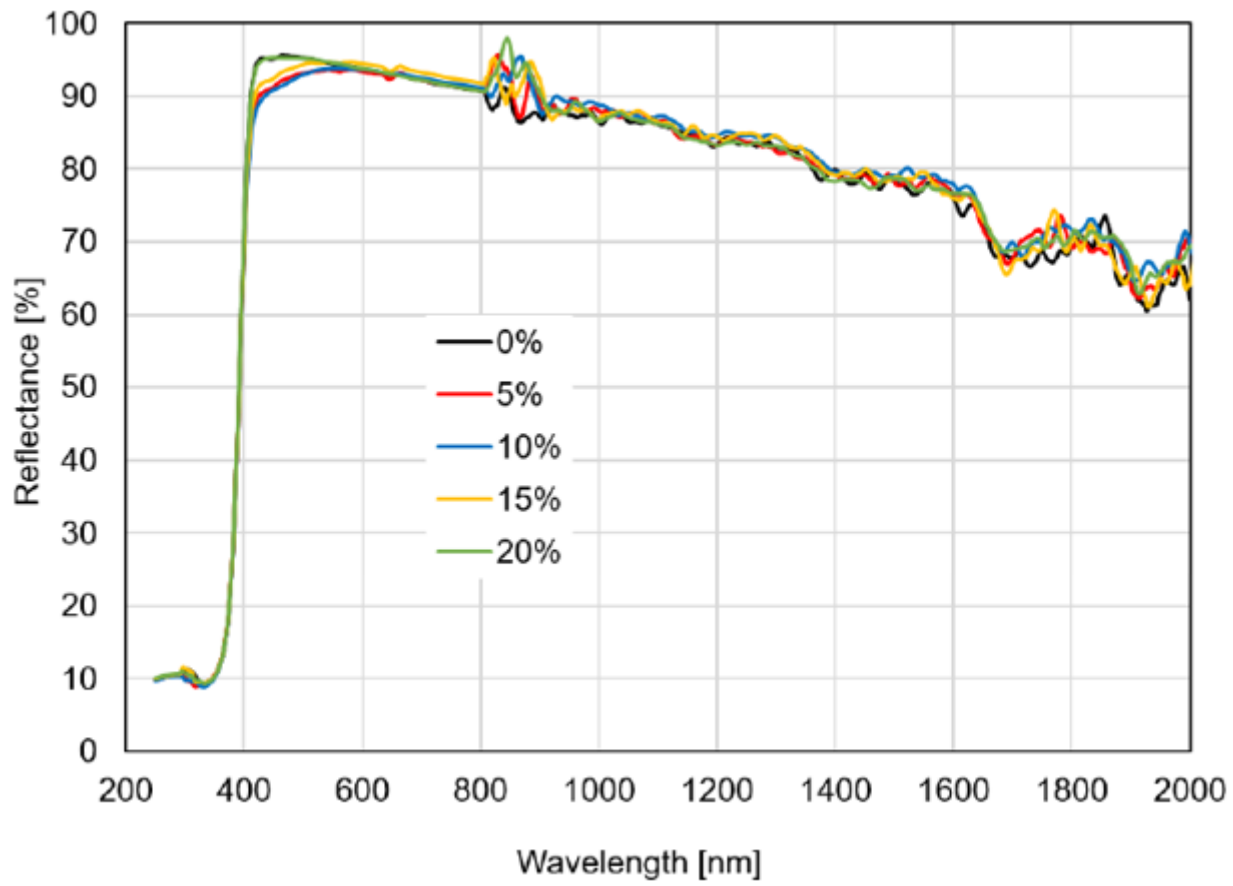


Figure 11

Spectral reflectance curves for paints with different SA content

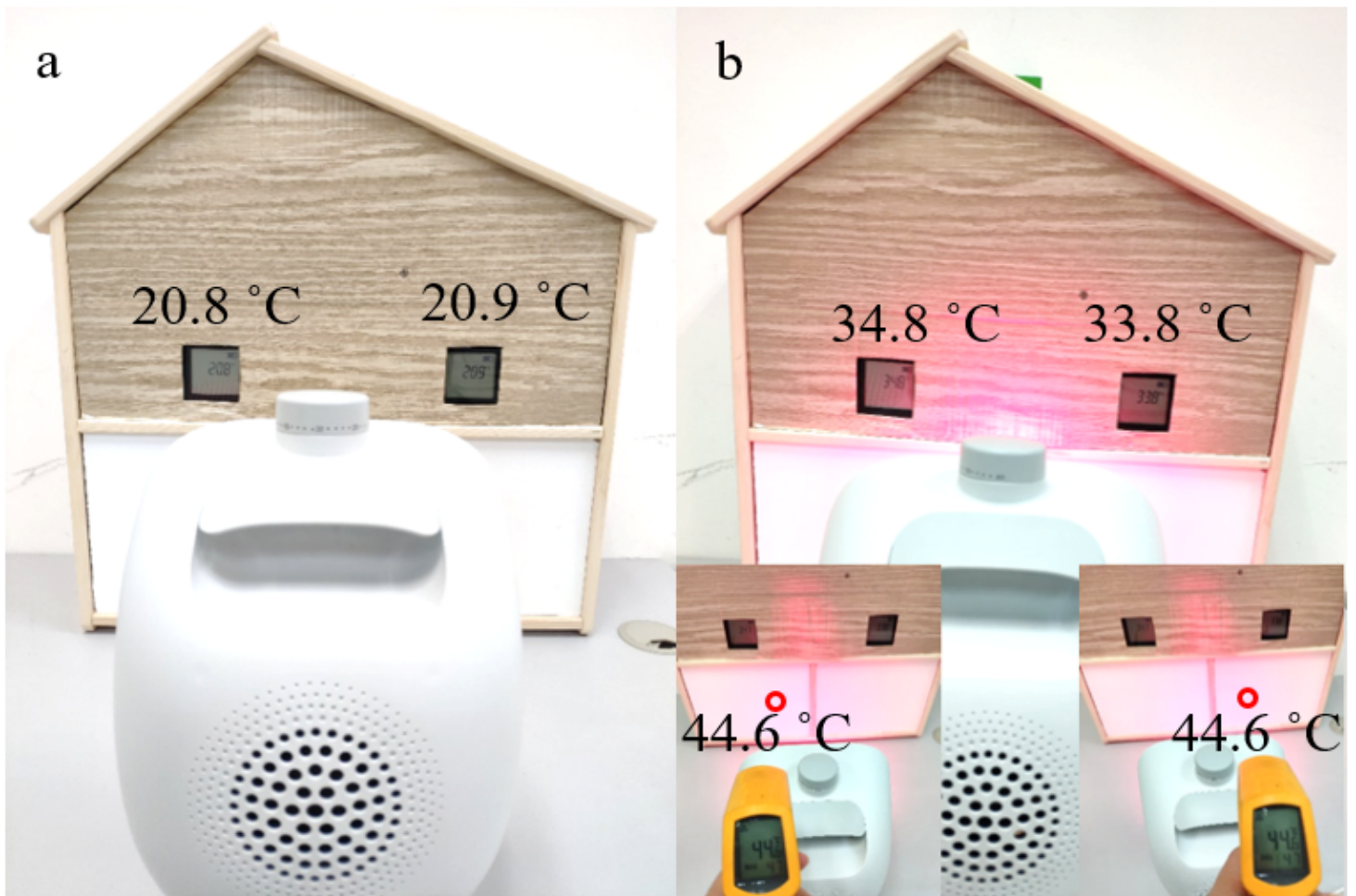


Figure 12

Thermal insulation performance of paints without (left) and with (right) 20% SA before (a) and after heating (b).

Supplementary Files

This is a list of supplementary files associated with this preprint. Click to download.

- [GraphicalAbstract.png](#)